Shuttling, swapping and mixing: the rapid modular evolution of antiviral repertoires in temperate phages and their satellites

Jorge Moura de Sousa[1*], Florence Depardieu[2], Marie Touchon[1], Raphaël Laurenceau[1,2], Kristen Curry[3], Alice Maestri[1], Florian Tesson[4], Arthur Loubat[4], Rayan Chikhi[3], Jean Cury[4], Aude Bernheim[4], David Bikard[2] and Eduardo P.C. Rocha[1*]

[1] Institut Pasteur, Université de Paris Cité, CNRS UMR3525, Microbial Evolutionary Genomics, Paris, France
[2] Institut Pasteur, Université de Paris Cité, CNRS UMR3525, Synthetic Biology, Paris, France
[3] Institut Pasteur, Université de Paris Cité, CNRS UMR3525, Sequence Bioinformatics, Paris, France
[4] Institut Pasteur, Université de Paris Cité, CNRS UMR3525, Molecular Diversity of Microbes, Paris, France

*Corresponding authors: jorge-andre.sousa@pasteur.fr; eduardo.rocha@pasteur.fr

ORCID IDs:
Jorge Moura de Sousa: 0000-0003-3530-8550
Florence Depardieu: 0000-0002-2680-0589
Marie Touchon: 0000-0001-7389-447X
Raphael Laurenceau: 0000-0002-1326-9928
Kristen Curry: 0000-0001-8375-397X
Alice Maestri: 0000-0002-2176-8831
Florian Tesson: 0000-0003-4038-1154
Arthur Loubat: 0009-0006-4647-4561
Rayan Chikhi: 0000-0003-1099-8735
Jean Cury: 0000-0002-6462-8783
Aude Bernheim: 0000-0003-0212-777X
David Bikard: 0000-0002-5729-1211
Eduardo P. C. Rocha: 0000-0001-7704-822X

Abstract

Interactions between bacteria, bacteriophages, and their satellites are shaped by a myriad of defence and counter-defence mechanisms. Here, we identified and characterized the defence hotspots of thousands of P2-like phages and P4-like satellites to elucidate the origins and evolutionary dynamics of defence systems. Both P4 and P2 encode a broad diversity of recognizable defence systems. Defences are a substantial, yet likely underestimated, share of the elements' pangenomes, as shown by novel antiviral functions discovered in P4 loci lacking known defence genes. Defence loci are very rapidly swapped, without pseudogenization, suggesting defences are replaced before becoming non-adaptive. This intense local recombination melds components of distinct systems into novel functional chimeras. Systems swap so rapidly that many elements with identical core genes have completely different defences. Surprisingly, despite P4 and P2's concomitant replication and packaging, they almost never exchange

defence genes. In contrast, near identical defence systems can be found in distinct types of MGEs and in cryptic chromosomal locations. Our findings highlight P4 and P2 as mobile platforms driving the modular diversification of bacterial antiviral repertoires. Hence, bacterial defences change quickly by phage and satellite turnover, and by the quick swap of defences within these elements.

Introduction

Microbial ecosystems are shaped by complex interactions between bacteria and bacteriophages (phages). These interactions range from the direct antagonism between virulent phages and bacteria[1] to the more nuanced continuum between antagonism and commensalism of temperate phages and their hosts, where the interests of both bacteria and phage can be aligned[2,3]. One key example of the latter is the presence of antiviral defences in prophages, which protect their host bacteria from predation by other phages, thus ensuring the survival of both[4,5]. Prophages are not the only mobile genetic elements (MGEs) that provide antiviral functions to their hosts. Anti-MGE defence systems are frequently encoded by MGEs present in bacterial genomes[6], possibly because of competition, and/or cooperation, between MGEs[7]. This is exemplified by phage satellites, non-autonomous mobile elements (hitchers) that hijack (helper) phages to mobilize between bacteria[8,9]. Some P4-like satellites encode antiviral defences against competitors of P2-like helper phages, protecting both helper and bacterial host[10]. Hence, the associations between satellites, phages and bacteria evolve in a mutualism-parasitism continuum, where partners incur in costs and benefits associated with the presence of the other elements[8].

The diversity of known defence systems is rapidly increasing. Defence genes have one of the highest rates of gain/loss across bacterial genomes[11], and in bacteria, their acquisition is typically associated with the mobility of the MGEs carrying them[12]. But little is known about the evolutionary dynamics of defence genes in MGEs themselves. Where do these genes come from, and how stable are they? What is the fate of these genes, and that of the MGEs carrying them, once defences are no longer useful? These questions are intricately linked not only with the ecology of MGEs (who is defending whom, when and against what), but also with their genomic organization, which for some elements like phages and satellites, can be tightly conserved[9,13,14]. The accumulation of accessory genes in phages is constrained by the size of their genomes, which must fit within their capsids[15], and the very modular genomic organization of both satellites and phages[9,14]. Although prophages often have accessory genes useful to their bacterial hosts, their high gene density suggests they rarely have pseudogenes and is thought to explain the low

frequency of transposable elements in their genomes, in contrast with plasmids[16]. Hence, the systematic detection of defence genes in prophages and satellites reflects the selective importance of these functions for their ecology and evolution. At a broader level, understanding the prevalence, localization and evolutionary dynamics of antiviral genes can highlight the rules that govern the genomic plasticity and genomic organization of MGEs, as well as their ecological associations and interactions with bacterial hosts and with other MGEs.

Several defence systems were previously detected in P2-like phages and P4-like satellites, in a single hotspot near the *cos* site of each element[10]. Here, we delimit satellite and phage genomes to identify additional hotspots and to account for MGE similarity when studying the evolutionary dynamics of antiviral genes within and across P4 satellites and P2 helpers. To extend the diversity of our dataset, we coupled the detection and precise delimitation of thousands of P4-like satellites[17] and P2-like prophages in complete bacterial genomes with thousands of additional P4-like satellites detected in metagenomes to generate the most abundant and diverse genomic collection of satellites and helper phages to date. The extensive dataset of P4 and P2 genomes allowed to uncover the quick turnover of defence genes encoded by P4 and P2, the genetic exchanges that underly this turnover, and how they shape defence repertoires.

102 **RESULTS**
103
104 ## Defence systems' loci are pervasive in a few hotspots of P2 and P4
105
106 We identified the P2-like prophages (P2 for short) and P4-like satellites (P4 for short) in
107 the complete genomes of *Escherichia coli, Klebsiella pneumoniae, Salmonella enterica*.
108 We also used the P4-like contigs detected in Logan, a repository of assembled sequence
109 data from tens of millions of public sequencing experiments[18], which greatly expanded
110 the number and genomic diversity of known P4 satellites (Fig S1, see Methods). The 3085
111 P4 (from complete bacterial genomes and metagenomes) and 1511 P2 (from complete
112 bacterial genomes) elements in our dataset were dereplicated and genetically delimited
113 at the nucleotide level by identification of their *att* sites (see Methods). We then identified
114 the defence systems in P4 and P2 using DefenseFinder[19] and PADLOC[20]. We also
115 searched for anti-defence systems, for which we only find two types (Anti_RM and
116 Anti_CRISPR) distributed in 28 P2. Most of these P2 have a single anti-antiviral system,
117 but one has five distinct systems. We detected no anti-defence systems in P4. Given the
118 low numbers of these anti-defence systems, we decided to exclude them from the main
119 analysis.
120
121 We found a very broad diversity of known types of defence systems, which occurred in
122 57% of P4 and in 49% of P2 (Fig 1A and B, Fig S2A for PADLOC classification). Some types
123 of systems were detected in both satellites and phages (e.g., AbiU or PD-T7-2), whereas
124 others were found in only one of them (e.g., AbiP2 in P2 and Hachiman in P4). We also
125 identified individual genes that are usually associated with defence systems, but that do
126 not form a complete known system (see the two rightmost columns in Fig 1A for systems
127 that were partially detected by DefenseFinder). We will refer to these as putative defence
128 systems and will explore them in more detail in a subsequent section. If we include both
129 complete and putative systems, the proportion of elements that encode defence-
130 associated genes increases to 73% (P4) and 81% (P2) (Fig 1B). Hence, a large majority of
131 these two types of MGEs encode genes associated with antiviral activity.
132
133 Even if this is by far the largest known dataset of P4 and P2, the pangenome saturation
134 curves show that we are far from having uncovered the full genetic diversity of these
135 elements (Fig 1C). Known defence genes correspond to a sizeable fraction of these

136 pangenomes (orange lines): 34% for P4 and 17% for P2. P4 and P2 account for 11-16% of
137 the genetic diversity of the defence systems in their hosts' species (Fig S3). Moreover, up
138 to 50% of the total defence systems of some genomes are encoded in their P4 or P2
139 elements (Fig 1D**,** Fig S4). This suggests that P4 and P2 are important contributors to the
140 defence repertoire of bacteria.
141
142 Most defence systems in P4 are in a hotspot between the integrase and Psu-Delta-Sid,
143 whilst many of the defence systems in P2 are in a hotspot between the primase (GpA) and
144 the portal (GpQ) (Fig 1E). These are the two previously described hotspots[10]. However,
145 other less populated defence hotspots exist between the primase and one of the *att* sites
146 of P4 (7% of the systems in P4), between the integrase and the *att* site of P2 (3% of the
147 systems in P2), between the integrase and the primase in P2 (8% of the systems in P2)
148 and within the late genes of P2. Although it is atypical for integrated elements to mobilize
149 genes between *att* sites and the integrase, this was previously observed for defence
150 systems of PICI[21]. An additional P2 defence hotspot was found downstream of GpL (16%
151 of the systems in P2), consistent with previous descriptions of a hotspot of accessory
152 genes within the tail genes in the classical P2 phage[22]. Moreover, some of these P2
153 defence hotspots correspond to known integration sites of horizontally transferred genes
154 in P2[23], and to the hotspots of accessory genes described recently in more than 1000 P2-
155 like phages[24]. In either P4 or P2, some defence systems were consistently found in a
156 single hotspot, whilst others were found across genomic locations of the elements (Fig
157 S5A). Of the P2 with complete defence systems, 10% have multiple defence systems
158 across different hotspots (Fig S2C, see also genomes in Fig 1E for examples). This fraction
159 is much lower for P4 (1%), suggesting that the accumulation of multiple defence systems
160 occurs more often in the larger genomes of P2. These results confirm that whilst defence
161 systems are very abundant and diverse in P4 and P2, representing a large fraction of their
162 accessory genes, they are encoded in a small number of genomic locations.

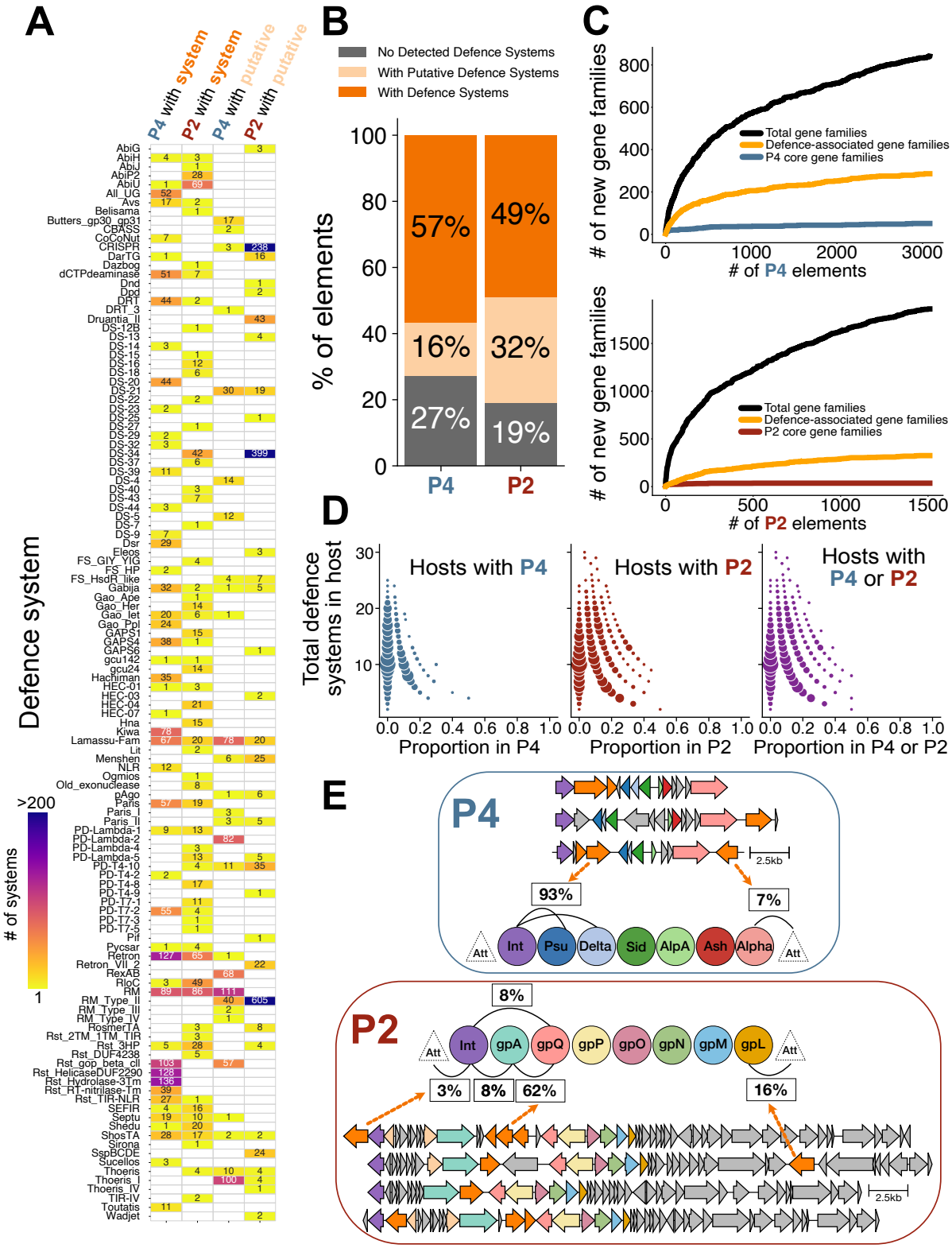

Figure 1. Abundance, distribution and localization of defence systems in P4-like satellites and in P2-like prophages. A. Number of the different types of complete (two leftmost columns) and putative (two rightmost columns) defence systems detected by DefenseFinder in P4 (1st and 3rd column) and P2 (2nd and 4th column). Darker colours in the heatmap correspond to higher numbers of systems. **B.** The proportion of P4 and P2 elements with defence systems deemed complete (orange, as detected by DefenseFinder or

PADLOC) or putative (light orange, detected by DefenseFinder). **C.** The pangenome (black) of P4-like satellites (top) and P2-like phages (bottom) with the relative contributions of the core (blue for P4, red for P2) and the defence-associated genes (orange). **D.** Fraction of systems (detected by DefenseFinder) of the host encoded in its P4 and P2 elements. The proportions of complete defence systems encoded by P4 in hosts that have at least one P4 (leftmost panel), encoded by P2 in hosts that have at least one P2 (middle panel), or encoded either by P4 or P2 in hosts that have at least one of either element (rightmost panel) are shown in the x-axis. The size of the circles corresponds to the frequency of each (x,y) pair. **E.** Distribution of defence systems in hotspots of P4-like satellites (top) and P2-like prophages (bottom). Hotspots are defined as locations among successive core gene families and are indicated by the edges in the graphs (% indicates the proportion of defence systems at these locations). When the core genes are not successive, it reflects cases where either one of the core genes is missing, or the cores genes are arranged differently from the prototypical organization of their respective element. Colour codes in genetic loci and graphs coincide; orange indicating complete and light orange indicating putative defence systems. Grey indicates genes that are neither core nor defence-associated.

Rapid turnover of defence systems

We then enquired on the turnover of the defence systems, i.e. how frequently closely related elements differ in the systems they encode. The phylogenies of P4 and P2 elements, based on their core genes (see Methods), show highly similar elements often carrying unrelated defences (Fig 2A and D). This can best be appreciated by focusing on the parts of the trees with many very similar elements and inspecting the diversity of systems they contain. To quantify this effect, we compared the gene repertoire relatedness (with wGRR, see Methods) of core genes and of defence genes between pairs of elements with defence systems. Consistent with the phylogenies, we observed an overwhelmingly large proportion of pairs of the same type of elements with non-homologous defence systems (99% in P4 and 99% in P2 pairs have wGRR defence<0.05). Since this includes pairs of very similar elements (i.e., with highly similar core genes) (Fig 2B and E, right panels), it shows that defence genes change very rapidly in both P4 and P2. We observed only a few pairs of dissimilar elements with similar defence systems suggesting that convergent acquisition of defences is rare (Fig 2B and E, left panels). These patterns remain qualitatively unchanged when comparing full genomes instead of core genes and when including the putative defence systems (Fig S6). If defence systems evolved in linkage with the core genomes of P4 and P2, we would expect a linear relationship between core and defence similarity, with deviations corresponding to

potential events of horizontal transfer of antiviral genes. Instead, the association between the evolution of defence systems and the core genes is almost null.

We then quantified the genetic linkage between defence genes and each individual core gene (Fig 1E). The Spearman correlations between the wGRR of defence genes and the sequence similarity of each core gene in pairs of P4 (Fig 2C and Fig S7A) and P2 (Fig 2F and Fig S7B) were all very low (≤0.2), in contrast to the correlations between core genes themselves. In summary, similar elements rarely encode similar defence genes and the latter show little genetic linkage with core genes. Both indicate very rapid turnover of defence systems in the genomes of P4 and P2.

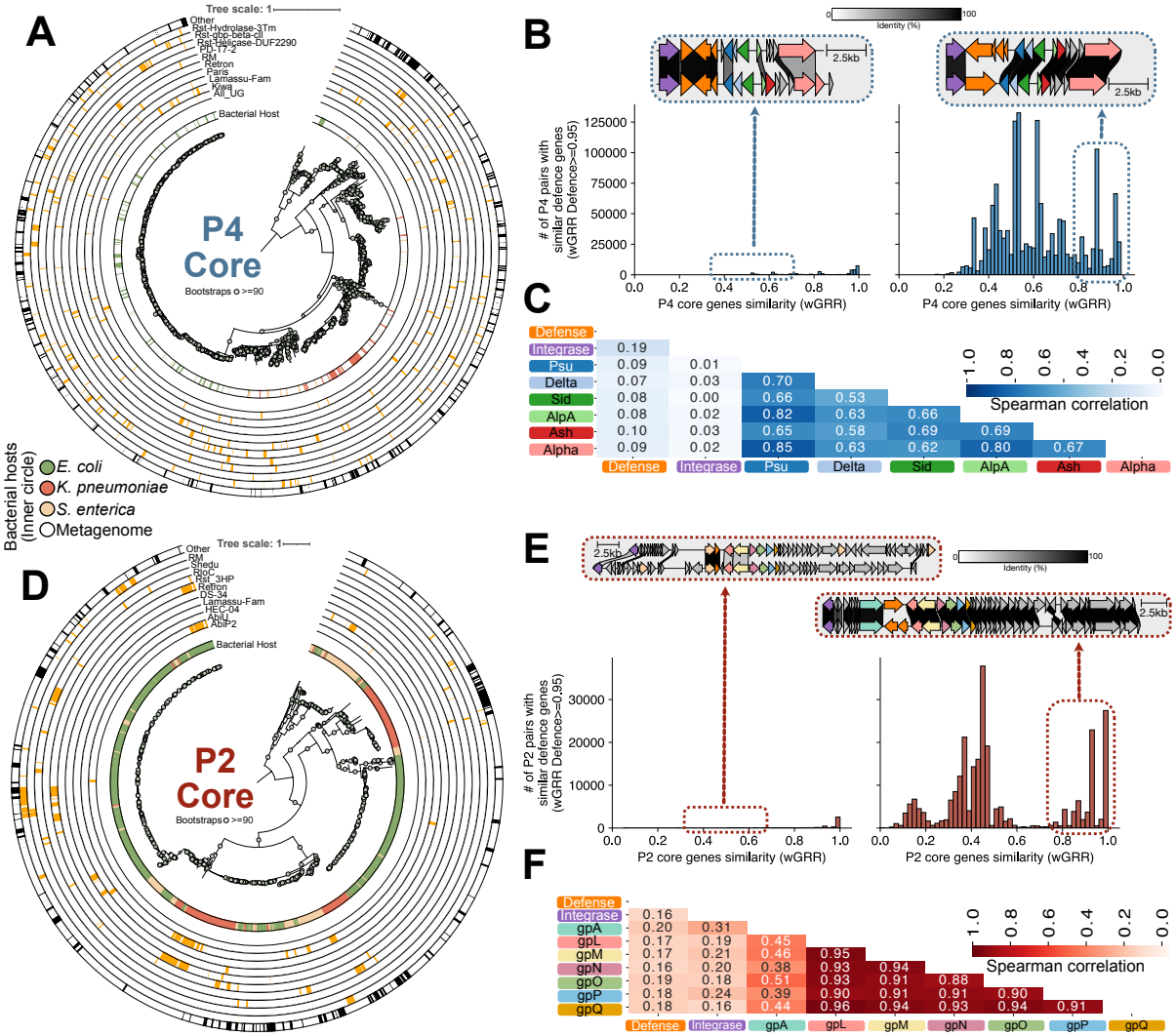

Figure 2. Relationship between antiviral repertoires and the core genomes of P4 and P2. A. Phylogeny of core genes of P4. Bootstraps of at least 90 are indicated with a circle (the larger the circle, the higher the bootstrap value). Colours in the innermost circle indicate the bacterial host of each P4 (white spaces

220 indicate P4 from metagenomes, without an assigned host). Note that since these are dereplicated P4
221 genomes, some P4 might be representative of a group of elements with multiple bacterial hosts (we
222 consider only the host of the representative genome). The ten outward circles represent the presence
223 (orange) or absence (white) of the ten most frequent defence systems in P4 (complete defence systems,
224 from DefenseFinder). The outermost circle indicates whether each P4 element has any other complete
225 defence system, apart from the ten most frequent in the family of elements (black shows cases where
226 another defence system is present). **B.** Left, number of pairs of P4 genomes with similar defence genes
227 (wGRR≥0.95) in function of the similarity between core genes (x-axis). Right, number of pairs of P4 genomes
228 with distinct defence genes (wGRR≤0.05) in function of the similarity between core genes (x-axis). **C.**
229 Spearman correlation values between the wGRR of defence genes and the bitscore values from BlastP of
230 individual core genes of P4-like satellites, for the set of all pairs of P4s. Colours of a stronger shade indicate
231 higher Spearman correlation values. **E.** Same as in A, but for P2 genomes and their defence systems. **F.**
232 Same as in **B**, but for P2 genomes. **G.** Same as in **C**, but for the defence and core genes of P2-like phages.
233
234 ## Pseudogenes of defence systems are rare in P4 and P2
235
236 Turnover of defence systems could occur in two ways. They could be first inactivated by
237 mutations or indels and subsequently replaced (Deletion-reacquisition model).
238 Alternatively, functional systems could be swapped by others before becoming defective
239 (Swap model). The first scenario suggests that systems are lost because they are not
240 selected for anymore, i.e., they are nearly neutral or even deleterious (costs outweigh
241 gains). The second scenario only requires that the new defence system is at least as
242 adaptive as the old one in the current population context. These models have different
243 testable predictions. The deletion-reacquisition model predicts the frequent presence of
244 pseudogenes of defence systems whereas the swap model predicts the opposite. We
245 assessed the fraction, type, and past function of pseudogenes in P4 and P2 using
246 PseudoFinder[25] (see Methods). The vast majority of P4 and P2 have at least one
247 pseudogene (94% and 98%, respectively, Fig 3), showing that defective genes remain long
248 enough to be identifiable in large numbers in these genomes. We note that, in some
249 cases, several identified pseudogenes can originate from a single gene. Although
250 pseudogenes are frequently found in defence-associated loci (Fig S8), only a very small
251 percentage of them had sequence similarity with defence-associated genes (less than
252 1% in P4 and c.a. 2% in P2). Many more had sequence similarity to core genes (24% in P4,
253 typically Ash pseudogenes) and especially to unknown function genes (Fig 3 insets, see

File S1 for PFAM annotations). These results suggest that defence systems are frequently swapped before being inactivated. Moreover, most pseudogenes in P4 and P2 are detected as very small intergenic sequences (c.a. 90% in either P4 or P2, Fig S9), which confirms that the putative defence systems detected in these elements are intact, likely functional genes.

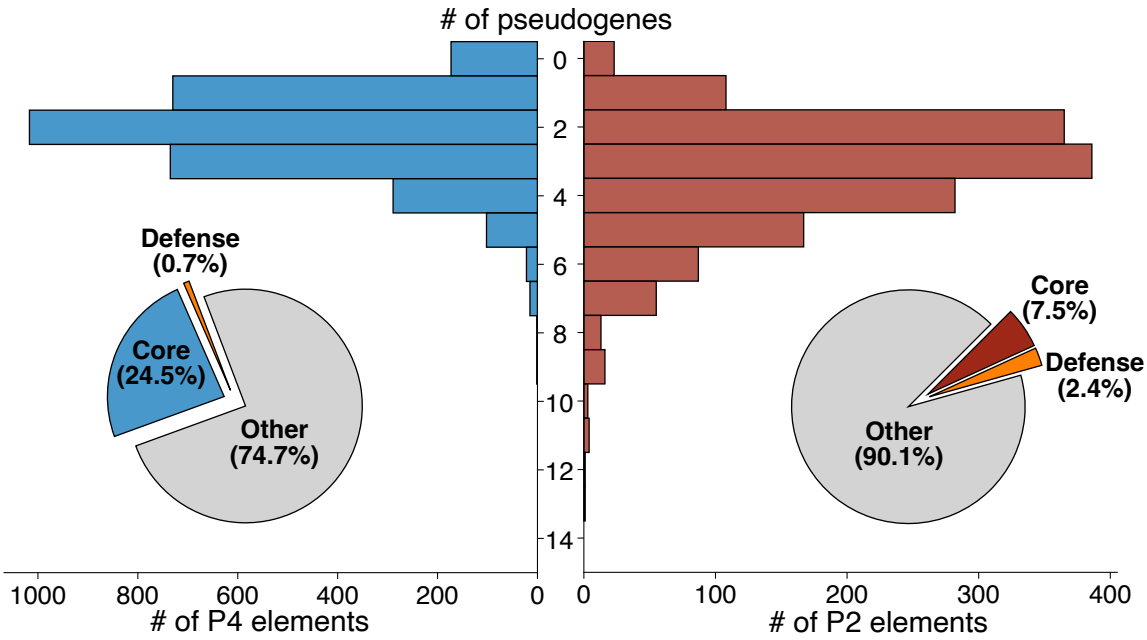

Figure 3. Quantification and characterization of pseudogenes in P4-like satellites and P2-like prophages. Histograms show the distribution of pseudogenes detected by PseudoFinder per P4-like satellite (left) and P2-like prophage (right). The charts as insets show the proportion of the pseudogenes annotated as defence (orange), core of each element (blue and red for P4 and P2, respectively), or with other (or no) annotations (grey).

P4 hotspots contain numerous novel or chimeric defence systems

We found many genes of defence systems that lacked the typical cognate components in the defence hotspots (Fig S5B). These could be inactivated systems, but our observation that pseudogenes of defence systems are rare make this hypothesis unlikely. Instead, they might be functional novel systems resulting from re-assembly of others[26,27]. To test this hypothesis, we selected 11 candidate systems based on their different characteristics (Fig 4, see File S2 for a description of the putative systems): some are potential variants of known systems (e.g., a Lamassu system missing a known effector);

279 others are mixtures of genes from different systems (e.g., two genes from the PD Lambda
280 2 system, and another from the Rst_gop_cll system); and others are potential
281 minimizations of known systems (e.g., a Thoeris system with a single ThsA gene). We
282 synthesized and cloned each putative system in a low copy plasmid under the control of
283 a pTet promoter, which were introduced into *E. coli* MG1655. An empty plasmid was
284 transformed to the same background as a control. We then challenged these strains with
285 a collection of 28 virulent phages to test the antiviral protection of each putative defence
286 system (see Methods, Fig S10, File S2). 8 out of 11 provided protection against several
287 virulent phages (Fig 4, top 11 rows). Failure to observe protection can arise from multiple
288 causes. The most likely explanations are: (i) the defence system is functional but does
289 not target any of the 28 phages included in the present panel; or (ii) the system is
290 functional in its native host but is not properly expressed, assembled, or active in the
291 heterologous *E. coli* host used here. Interestingly, a system similar to the Lamassu
292 variant, which did not provide protection against the phages tested here, was recently
293 shown to be provide an anti-phage function[28]. The high success rate we obtained in
294 detecting resistance against this limited phage panel strongly suggests that most of the
295 putative systems not recognized as complete by either DefenseFinder or PADLOC are
296 functional.
297
298 Some P4 (27%) and P2 (19%) lack identifiable defence genes (Fig 1B) but have genes of
299 unknown function at their main defence loci. We hypothesised that some of these could
300 be novel antiviral systems. We selected at random 8 P4 satellites with genes of unknown
301 function to test their anti-phage phenotypes, as above (Fig 4, bottom 8 rows, Fig S10). 6
302 out the 8 conferred protection against multiple virulent phages. phages. As previously,
303 this high success rate indicates that most of these unannotated loci are likely *bona fide*,
304 functional defence systems. We named the novel functional systems according to deities
305 from Lusitanian mythology, while waiting for a uniform standardised system of
306 nomenclature, and they are described in detail in File S3.
307
308 When possible, we characterized the novel systems using available data, sensitive
309 sequence similarity detection programs (wjth HHPred), and structural similarity (with
310 ESMFold and FoldSeek, File S3). The Crouga system has some evidence of being an RM-

like system, with one of its proteins containing PFAM domains (ResIII, DEAD and Helicase C) associated with other RM systems[29]. The Bandua system has two proteins with domains typically associated with immune functions (a nuclease and a kinase, respectively). Neither protein is recognized by current antiviral annotation pipelines. The Aernus system has one protein annotated with kinase and nuclease domains, and a second one annotated as a mannitol repressor. It is unknown at this point if the latter has any impact in antiviral capabilities. The single protein in the Toga system has several hits with protein domains associated (through FoldSeek) with the Gao_Ppl[30] and the SMC defence systems[31], albeit not being recognized by any of the current models for either system. The Reve system is another single gene system, with ATPase and KAP family P-loop domains[32]. Finally, the last system we tested has two proteins, one with pentapeptide repeats and an IRK potassium channel domain, which could be involved in membrane depolarization, while the other protein contains a Nucleotidyltransferase like domain and a HEPN-like domain, suggesting it acts on host or phage RNA. A system with similar components was described by others during the course of this study as Hailong[33], which is currently not detected by DefenseFinder or PADLOC. Hence, and despite being part of the non-defence annotated genes in P4, we refer to it as Hailong to avoid introducing redundant nomenclature.

The novel systems described above, together with the unannotated Hailong system, are clear evidence that at least some genes of unknown function in P4 have antiviral phenotypes, with most (e.g., Bandua, Aernus, Toga and Reve) providing strong protection against Drexlerviridae and/or Siphoviridae phages). We thus wondered whether other genes in the defence-less elements could have similar properties. For this, we collected all the genes of unknown function from P2 and P4 detected only in complete genomes, to use the information on their larger chromosomal context, and analysed them using a recent machine learning approach to detect antiviral domains (see Methods). We observed a significant signal for the association of antiviral defences in 30% of the proteins of unknown function in P4 (62%, with the method that considers the genomic context), and in 15% of the unknown proteins in P2 (32%, with the method that considers the genomic context) (Fig S11). We note that all the confirmed novel systems are part of those predicted to have an antiviral function, due to their genetic context. The

computational predictions, together with experimental validations, demonstrate that P4-like satellites constitute major loci for both established and yet-to-be-discovered functional defence systems. Moreover, many of the proteins of unknown function that cluster in P4- and P2-associated defence hotspots are predicted to encode antiviral activities.

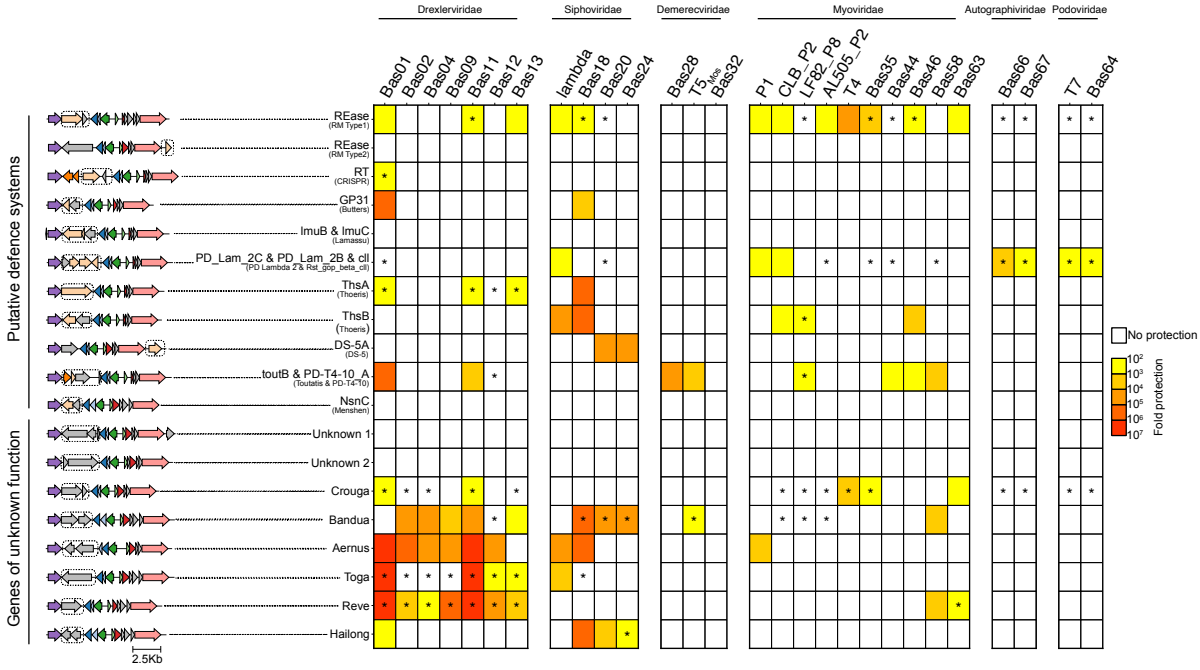

Figure 4. Putative and unknown defence systems in P4 provide protection against phage infection. On the left are the genomes of P4 with putative defence systems (light orange genes, top 11 rows) and the genomes of P4 with genes of unknown function in their defence loci (grey genes, bottom 8 rows). For the former, the names of the genes, as well as the complete systems with which they are associated, are shown in front of each genome. The regions synthetized in plasmids are boxed (exact sequences in Datasets E1 and E2). Heatmap of the phage resistance phenotype shows the mean fold resistance of two independent replicates of each putative and unknown system against a panel of 28 *E. coli* phages. The degree of protection is indicated by the colour (log) scale, with darker red colours indicating higher levels of protection, relative to the same bacterial background with an empty plasmid. Only the infections where both replicates show increased protection, and the mean of the two replicates is ≥ 10-fold difference, are shown as coloured squares. Asterisks indicate smaller plaque morphologies, relative to the infection of the strain with the empty plasmid. Plaque-forming units were measured for each phage on cells harbouring either a control plasmid or a defence system (Fig S10). Fold-resistance was calculated as the ratio between these two values. All systems were expressed from pTet promoter in the presence of anhydrotetracycline (aTc, 0.5 µg/ml) and measured at 37°C, except for T7-like phages, which were measured at room temperature. The raw data for the ratios system/control are shown in File S4.

368
369 ## P4 and P2 exchange defences with other MGEs but not with each other
370
371 If defence systems are constantly swapped in both P4 and P2, where do these genes
372 come from? To address this question, we searched for closely related homologs (>85%
373 identity, see Methods) of defence genes from either P4 or P2 in 32798 bacterial and in
374 27022 phage genomes. For 6% of defence genes in P4, and for 2% of the defence genes
375 in P2, we found at most one homolog, indicating that some of these defence genes are
376 likely variants specific to the P4 and P2 in our dataset (Fig S12). Many of the remaining P4
377 and P2 defence genes have homologs in multiple genomic contexts (Fig 5A). Similar
378 results were found when including the putative novel defence systems from the first
379 section (File S5, Fig S13). To avoid comparing elements that might have similar systems
380 because of recent common ancestry, we excluded the pairs of very similar (wGRR>=0.95)
381 P4 or P2 elements. Nevertheless, the analysis reveals that most homologs of defence
382 genes of P4 (76%) and P2 (47%) are in bacterial regions predicted to be respectively P4-
383 like satellites and P2 phages. These include P4 and P2 in bacterial hosts (e.g.,
384 *Citrobacter*, *Enterobacter* or *Pectobacterium*, Fig S14) where these elements'
385 delimitation in bacterial chromosomes was not possible for lack of information on their
386 *att* sites (called P2* and P4*, see Methods). These elements had hence not been included
387 in our focal dataset of phages and satellites. P2 and P4 often co-occur in genomes and
388 are induced and replicated at the same time. One could thus expect that they would
389 exchange defence systems. Surprisingly, we found only one case of closely related
390 defence genes between P4 and P2, even when including all putative defence systems (Fig
391 S15). Hence, hitchers and helpers have not recently exchanged defence systems.
392
393 The highly similar homologs of P4 and P2 defence genes found in bacterial regions that
394 are not identified as P4 or P2-like could be the result of recent genetic exchanges with
395 other MGEs. We found no homologs in the other families of satellites known in
396 Enterobacteria (PICI and cfPICI[9,17],File S5). Both P4 and P2 defence homologs were found
397 in (non-P2 like) prophages, albeit this was much more frequent for P2, which also has
398 defence homologs in 31 temperate and 11 virulent phage genomes (all P2-like).
399 Chromosomal regions with integrative conjugative elements[34], which are known to
400 encode antiviral systems[35], account for very few of the homologs of P4 or P2 defence

genes. P4 and especially P2 defence systems have relatively more homologs in plasmids. Some of the latter could correspond to phage-plasmids (P-Ps), since they are plasmid replicons identified as phages by geNomad[36], although they are not part of the current dataset of known P-Ps[37]. The MGEs and bacterial regions with homologs of defence genes of P4 and P2 are sometimes within bacteria that are phylogenetically distant from the hosts of P4 and P2, such as *Pseudomonas* or *Vibrio* (Fig S14). These results suggest that exchange of defence systems tends to occur between similar types of elements, but can also involve distinct MGEs.

Genetic exchanges with other MGEs may allow to introduce novel types of defences in P2 or P4, which can then be exchanged within each group of elements. For instance, the phylogeny of a variant of the AVS_V system, detected in P2 from *K. pneumoniae*, includes homologs in non-P2 prophages and uncharacteristic genomic regions from different bacterial hosts, that form a separate clade (Fig 5B). Intermingled with the two main clades are two terminal branches, corresponding to an uncharacteristic genomic region in *Proteus* and a single plasmid in *Duffyella*. The phylogeny suggests the acquisition of the system by P2 was recent. It was then followed by the dissemination of this variant of AVS_V within *K. pneumoniae* in P2 phages. Another defence system detected in P2, Lit, is mostly found in plasmids and uncharacteristic genomic regions. While being rare in prophages, a homolog is found in a single P2-like prophage (Fig S16A). Given its singularity, and the scarcity of this type of systems in P2 (Fig 1A), this likely illustrates a recent acquisition of the Lit system by this P2.

Exchange of defence systems between different types of MGEs also broadens the mechanisms of dissemination of the former within bacterial species. For instance, the phylogeny of a variant of the PD-T7-2 A is consistent with a unique, recent exchange of this system between P4 and plasmids (whose direction cannot be ascertained from this data alone). The system in the plasmids has diversified in two separate genetic variants that disseminated in *K. pneumoniae* (Fig 5C). The phylogeny of the other gene of the system (PD-T7-2 B) shows yet another variant in P4 that is disseminating the defence system in *Escherichia* and *Klebsiella* hosts, with a transfer to plasmids in the latter (Fig S16B). Hence, events of exchange between MGEs show the establishment and further

433 diversification of defence homologs in different MGEs, allowing the spread of defence
434 systems within and across species through different mechanisms of horizontal gene
435 transfer.

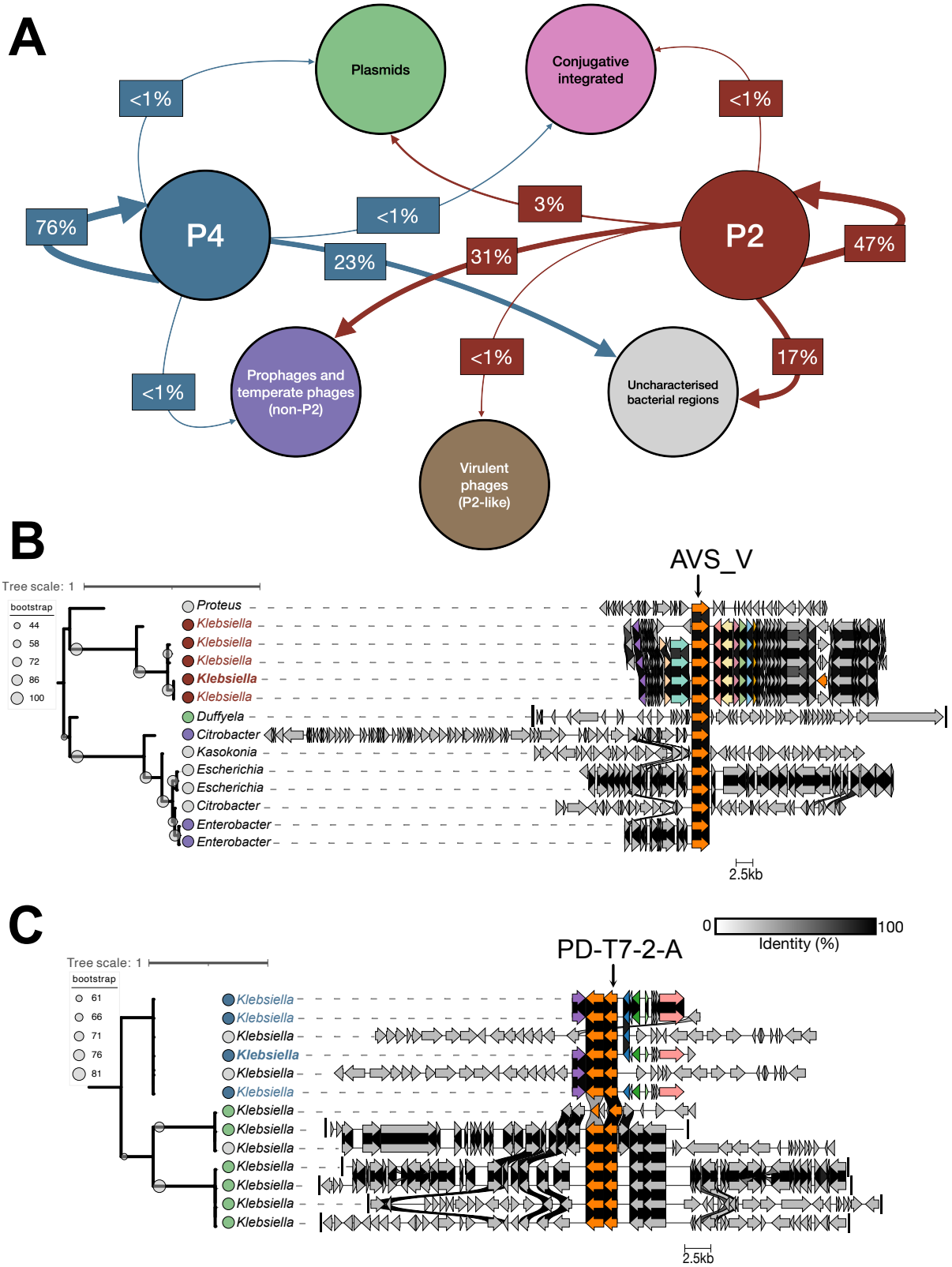

436

Figure 5. Highly similar homologs of defence genes of P4 and P2 are found in completely different genomic contexts. A. Graph based representation of the number of instances where homologs of defence genes (from complete defence systems) in P4 and P2 are found in different genomic contexts. These include other MGEs (plasmids, phage-plasmids, conjugative integrated elements, prophages and virulent phages) or regions of the bacterial genomes that are uncharacteristic. Thickness of the arrows represents the proportion of homologous matches detected between defence genes from P4 or P2 and the other different genomic contexts (thicker arrows correspond to a higher proportion of matches). The exact values for each combination are shown in File S5. **B.** Phylogeny of the AVS_V gene, comprised of the gene found as a defence system in a focal P2 in *Klebsiella*, and its homologs detected in either other P2s (red circles at the tree leaves), plasmids (green circles), prophages (violet circles) or uncharacteristic genomic regions (grey circles). The genes corresponding to each of the elements (or to the segments that include the uncharacteristic genomic regions as grey circles) are shown in front of the tree, with larger plasmids truncated for visibility. **C.** Phylogeny of the PD-T7-2-A gene, comprised of the gene found in a PD-T7-2 defence system in a focal P4 in *Klebsiella*, and its homologs detected in either other P4s (blue circles at the tree leaves), plasmids or uncharacteristic genomic regions. The genes corresponding to each of the elements (or to the segments that include the uncharacteristic genomic regions) are shown in front of the tree, with larger plasmids truncated for visibility.

Cryptic genomic islands have homologs of defence genes from P4 and P2

A large fraction of homologs of P4s or P2s identifiable defence systems are found in bacterial uncharacteristic genomic regions (UGRs) that do not correspond to known MGEs. Their genomic context (20 genes each side) often contained tRNAs genes, which are well-known points of integration of MGEs[38] (Fig S17A). Functional annotation with EggNOG Mapper and PFAM revealed that some of these genes are typical from P4 or prophages (Fig S17C and D, see blue and red dots). These regions also contained many pseudogenes of proteins typical of MGEs (Fig S17A and B). Since these results suggested that some UGRs could be defective satellites or phages, we systematically annotated them using the core markers of P4 and P2 (see Methods) and PseudoFinder. In total, 745 URGs encode highly similar homologs of bacterial antiviral genes detected in P4s (Fig 6A, File S5) and many of them (27%) have at least one P4-specific marker(s). All 745 UGRs have at least one pseudogene, and about half have pseudogenes (typically intergenic) homologous to a P4 core gene. Conversely, in the 775 UGRs that encode highly similar homologs of bacterial defence genes detected in P2s, P2-like markers are found in ca. 20% of them. Although almost all (>98%) of these UGRs have at least one pseudogene,

473 only 5% of them correspond to a P2-like core gene. The above observations remain
474 qualitatively similar when including the putative defence systems (Fig S18). UGRs with P4
475 or P2 core markers are thus very likely defective versions of these elements. Within them,
476 we found numerous pseudogenes of mobility functions, but the neighbouring defence
477 genes remained almost identical to those of intact elements, and are thus likely
478 functional (Fig 6B-C). These results mean that defective P4 and P2 either engaged in
479 genetic exchanges of defence systems with their functional counterparts, or are non-
480 mobile satellites and prophages with stabilized (and conserved) defence genes.
481 Moreover, and consistent with the absence of genetic exchanges between hitcher and
482 helper (Fig 5), homologs of defence genes in P4 and P2 are also not found in defective
483 elements of the opposite type.
484
485 Almost 50% of UGRs with homologs to P4 defences and 80% of the UGRs with homologs
486 to P2 defences lack any P4- and P2-specific markers, considering both the genes and
487 pseudogenes within these regions. They are thus cryptic genomic islands, completely
488 distinct from P4/P2, and of unknown mobility. The detection of defence homologs in such
489 dissimilar islands is consistent with the observed putative exchanges of P4 and P2
490 defences with MGEs of different types, where we do not expect to find large regions of
491 homology (Fig 5).
492

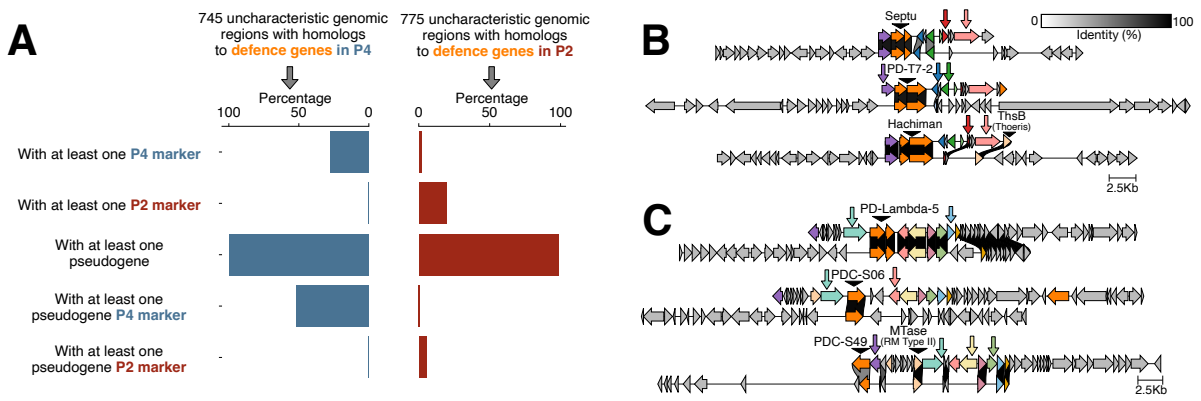

493
494
495 **Figure 6. Quantification of pseudogenes and P4-like/P2-like markers in uncharacteristic genomic**
496 **regions with homologs to defence genes encoded by P4 and P2. A.** Characterization of uncharacteristic
497 genomic regions (URGs) that encode homologs to defence genes found in P4 (left bars, blue) and URGs
498 that encode homologs to defence genes found in P2 (right bars, red). We quantified the proportion of these
499 URGs that encode P4/P2 markers predicted as pseudogenes by PseudoFinder (last two bars). **B.** Examples
500 of P4-like satellites, and the homology of their defence systems with URGs that contain incomplete (likely

defective) P4-like satellites. In each genomic comparison, the coloured arrows indicate P4-like core genes that were detected as intergenic pseudogenes in the URGs. **C.** Examples of P2-like prophages, and the homology of their defence systems with URGs that contain incomplete (likely defective) P2-like prophages. In each genomic comparison, the coloured arrows indicate P2-like core genes that were detected as intergenic pseudogenes in the genomic regions.

507 ## DISCUSSION

508

509 The systematic detection of defence genes in prophages and satellites is a strong
510 statement on the selective importance of antiviral functions for the ecology and evolution
511 of these MGEs. Given the prevalence of P4 and P2 in Enterobacteria[17], and the large
512 proportion of their accessory genes that we show here to be dedicated to defence, these
513 MGEs constitute a significant fraction the bacterial repertoire of defences. Yet, the
514 elements' pangenome dynamics show that the sampling of their natural diversity is not
515 yet exhausted, even when considering, for the first time, the vast diversity of P4 elements
516 in metagenomes using Logan[18]. Our experimental validation of anti-phage activity for 13
517 novel systems encoded by P4 confirms that the contribution of defence functions to the
518 pangenomes of P4 and P2, as well as to the antiviral repertoire of their bacterial hosts,
519 will keep surprising us.

520

521 The diversity of antiviral functions in P4 and P2 is driven by events of genetic swaps at
522 defence-specific hotspots, enlightening the underlying processes of natural selection in
523 MGE-defence associations. A novel system will fix in a population of MGEs if it has
524 adaptive value. Targeted phages may, over time, adapt to resist this novel system,
525 reducing the selective advantage of retaining it in the MGE genome. It has remained
526 unclear if this process typically runs until the defence systems become neutral (or even
527 deleterious, e.g., due to autoimmunity[39]) or if defences are replaced beforehand. Our
528 observation of rapid replacement of the systems and the lack of defence-associated
529 pseudogenes at these loci suggest that recombination quickly swaps functional systems
530 without the latter passing by a period of inactivation. Although many small intergenic
531 regions predicted as pseudogenes are in defence loci, they are likely remnants of an
532 intense process of recombination. What little may remain of antiviral genes in these
533 regions lost any recognisable homology with known defences, even if they could
534 potentially give rise to novel defence genes[40]. These findings have two implications. First,
535 defence systems may be lost when they are still adaptive: it suffices that the novel system
536 is more adaptive for the swap to be fixed in the population by natural selection. Second,
537 it suggests that systems spend little time, if any, as neutral components of the MGE
538 genome.

P4 and P2 exchange their defence systems with elements of the same type and, less frequently, with other MGEs. Yet, they do not exchange with each other. This is puzzling because P4 and P2 frequently co-occur within bacterial hosts, and are co-induced, replicate and package their DNA simultaneously[41]. This should provide plenty of opportunities for genetic exchanges[9,42], particularly since phage induction, replication and recombination are mechanistically concomitant[43,44]. Three factors may explain this result. First, exchanges by homologous recombination require high sequence identity that is lacking between P2 and P4[45]. Yet, we do observe exchanges between these elements and other unrelated MGEs, like plasmids. Second, because P4 and P2 often co-occur in genomes, there might be selection against the presence of redundant defences in the two elements. Different types of defences in P2 and P4 would maximize the range of anti-phage defence of the consortium. Identical defences would be redundant, and one set could be easily lost by genetic drift. Third, if P2 have defence systems to prevent P4 infection, or to avoid the hijacking of P2 particles by P4, these systems might be counter-selected in P4. Conversely, P4 might carry defence systems that increase the fitness of P4 by decreasing the ability of P2 to use its own capsids. If they exist, such genes are not expected to be acquired by P2 phages.

Despite the lack of exchanges between P2 and P4, we found very similar defence systems in distinct MGEs or genomic islands, suggesting that genetic exchanges between very different elements is possible. It is difficult to estimate the direction of these exchanges, although in some cases the defence was very likely acquired by P4 or P2 from other MGEs. When a phage or a satellite acquires a defence gene from a plasmid, the system can now be exchanged more easily with other satellites or phages[46]. These exchanges can also contribute to the flow of antiviral genes between phylogenetically distant bacteria, if the MGEs involved in these exchanges have different host ranges. We also found defence homologs in defective MGEs. It will be interesting to investigate if this corresponds to their domestication, resulting in the stabilization of the defence genes in bacterial genomes, or if defective elements still actively swap their defences with other MGEs.

571 Defence genes in P4 and P2 have evolutionary histories that are strikingly different from
572 the rest of the elements' genomes. Antiviral defences, in accordance with the idea that
573 they are "guns for hire", change genomic contexts of MGEs as quasi-independent
574 entities[47]. Yet, they do so in ways that resemble the change of bacterial chromosome
575 contexts by MGEs: frequent recombination breaks genetic linkage between defence
576 genes and the core genes of the elements, like MGEs are unlinked from the bacterial
577 chromosome lineage[48]; defence genes integrate predictable (hotspot) locations, like
578 MGEs in bacterial chromosomes[49] (through a presumably different mechanism); the
579 modularity of defence systems can promote the emergence of hybrids through
580 recombination, resembling the modularity of the evolution of prophages[50,51]; defence
581 genes are a large fraction of the satellite and the phage's pangenomes, similar to the
582 contribution of MGEs to bacterial pangenomes[52]; and defence genes provide accessory
583 functions to both phages and satellites, which in turn do the same to their bacterial
584 hosts[2]. The key difference is that defence systems are not known to encode mobilization
585 functions. Instead, our results suggest that P2 and P4 hotspots function as factories of
586 novel systems by recombination processes that still need to be elucidated. It also
587 remains to clarify how mutations and natural selection act on these chimeras to
588 eventually lead to their fixation as functional hybrid systems. In summary, our work
589 shows that P2 and P4 can be seen as genetic platforms that accumulate, diversify, and
590 then disseminate bacterial defence systems across microbial populations.

591 ## MATERIALS AND METHODS

592

593 ### Genomic and metagenomic datasets

594

595 We retrieved all the complete genomes of the NCBI non-redundant RefSeq database
596 (ftp://ftp.ncbi.nlm.nih.gov/genomes/refseq/, last accessed in May 2023), which consists
597 of 32799 complete bacterial genomes. The metagenomes used for the detection of P4-
598 elements were retrieved by aligning a query set of 538 clustered P4 protein sequences to
599 Logan v1.1 contigs using DIAMOND2[53], as described in the Logan manuscript[18]. We also
600 retrieved from GenBank a dataset with 27022 complete bacteriophage genomes
601 (retrieved March 2024). The lifestyle of each of these bacteriophages was inferred using
602 Bacphlip[54].

603

604 ### Identification and delimitation of genomic regions of P4-like satellites or P2-like
605 prophages in complete bacterial genomes

606

607 P4-like satellites were initially detected from the RefSeq bacterial genomes as described
608 previously[17]. This resulted in 3437 P4-like genomes of Type A or B. All prophages encoded
609 by bacterial genomes were detected using geNomad (version 1.5.2, default
610 parameters)[36]. In total, we detected 88288 prophages in the RefSeq bacterial genomes.
611 We then designed a MacSyFinder[55] model corresponding to a prototypical P2-like
612 prophage. The components of the model include the GpQ-L operon, which is conserved
613 in P2-like prophages[56], as well as an integrase and a primase (GpA). This model was
614 directly applied to the prophages detected by geNomad, resulting in 8165 P2-like
615 prophages of Type A, B or C. The latter two types of P2-like prophages are often missing
616 either the integrase, or the primase. We speculate that these two components are either
617 less conserved than the profiles used for the GpQ-L operon, or excluded by geNomad
618 during the predicted prophage region. The proteomes of these elements were retrieved
619 by extracting all the genes within the farthest core components. This general set of non-
620 att delimited 3437 P4-like satellites and 8165 P2-like prophages constitutes what we
621 name, respectively, the broad P4* and P2* categories.

622

623 A stricter definition of the genomic regions corresponding to P4 and P2 was achieved by
624 identifying *att* sites (attL and attR) at the borders of these elements in three bacterial
625 species, *Escherichia coli* (Ec), *Klebsiella pneumoniae* (Kp), and *Salmonella enterica* (Se),
626 which constitute the most abundant hosts of P4 and P2 elements[17]. To do so, we started
627 by identifying genomic spots containing P2 or P4 core genes across bacterial
628 chromosomes. The genomic positions of P4 and P2 elements described above were
629 mapped relative to persistent genes in the three host species (Ec: 2527 genomes, Kp:
630 1510 genomes, and Se:1256 genomes) to facilitate MGE delimitation and comparison
631 across genomes. The pangenome of each species (i.e., the full bacterial species gene
632 repertoire, not to be confused with the P2/P4 pangenome) was computed using the
633 pangenome module of PanACoTA v1.4.1-dev[57], applying a minimum sequence identity
634 and coverage threshold of 80%. Persistent gene families—those present in a single copy
635 in at least 90% of genomes—were extracted using the corepers module of PanACoTA.
636 Intervals were defined as the regions between two consecutive persistent genes within
637 genomes. P2 and P4 core genes are not persistent across species and are confined to
638 these intervals, providing an upper bound for their genomic positions. In total, 6,008
639 intervals containing P2 or P4 core genes (excluding integrases) were identified across the
640 three species (2258 in *Ec*, 2,66 in *Kp*, and 1384 in *Se*). Intervals from genomes of the same
641 species were grouped into genomic spots if flanked by the same pair of persistent gene
642 families, allowing comparison of equivalent regions across genomes. The number of
643 genomic spots occupied by P2 and P4 was generally low in each species (30 in *Ec*, 16 in
644 *Kp*, and 21 in *Se*).
645
646 P2 and P4 integrate the bacterial chromosome using a Tyrosine recombinase (integrase),
647 which mediates site-specific recombination between the host *attB* site and the MGE *attP*
648 site. Integration duplicates part of *attB* at the element edges, generating *attL* and *attR*[58],
649 which can be identified by sequence similarity within genomic spots. For each spot
650 described above, the shortest interval observed in the species was extracted as the
651 ancestral MGE-free state containing *attB*; when this assumption does not hold, *att* sites
652 cannot be reliably identified. Each such interval was then compared using sequence
653 alignments with longer intervals containing P2 or P4 elements, expected to harbour short
654 repeats of *attB* at their edges. To ensure at least two significant sequence alignments per

655 comparison and to account for possible integrations within persistent genes, intervals
656 were extracted including the flanking persistent genes and oriented so that these genes
657 point in the same direction, restricting the search to the positive strand for computational
658 efficiency. Sequence similarity between the shortest interval (query, *attB*) and each
659 longer interval (subject, candidate *attL/attR*) within the same spot was screened using
660 BLASTn of BLAST 2.9.0+[59] (-evalue 0.001 -strand plus). Alignments with ≥80% identity
661 were retained, and redundant hits fully contained within longer alignments were
662 discarded. Pairs of hits on the subject aligning to overlapping regions of the query were
663 interpreted as duplications associated with integration. The overlapping region on the
664 query defines the putative *attB* site, and the corresponding regions on the subject define
665 *attL* and *attR*. Pairs of *att* sites flanking all P4/P2 core genes were then selected to
666 precisely predict element boundaries, resulting in the delimitation of 2175 elements in
667 *Ec*, 2230 in *Kp*, and 1357 in *Se,* corresponding to 96 % of intervals containing P2/P4 core
668 genes. This approach does not rely on genomic context, such as the presence or position
669 of tyrosine recombinase genes (unlike methods such as TIGER[60]). Although integrases
670 were not considered while detecting P4 and P2 spots, they are present in nearly all
671 delimited elements – with only 76 exceptions - and in most cases (5638), the integrase is
672 located within 2kb of an element boundary, demonstrating the robustness of our method.
673 Att site pairs (sequences), element size, and integrase presence are provided in File S6.
674
675 From the P4/P2 intervals with an *att* identification, we further filtered the elements
676 according to their size (<20kb for P4 and <50kb for P2) and discarded P4 that were lacking
677 more than two core genes (i.e, only considered P4 of Type A or B, according to
678 SatelliteFinder). Delimiting and filtering the elements in the 3 main bacterial species,
679 resulted in a total of 2168 P4-like satellites and 3574 P2-like prophages originating from
680 complete bacterial genomes.
681
682 Identification and delimitation of genomic regions of metagenomes that correspond to
683 P4-like satellites
684
685 To detect P4-like satellites in the metagenomic contigs, the latter were initially processed
686 as described previously in[18]. The 7 P4 core genes were detected in a set of 210895 "P4-

687 like contigs". An initial step of dereplication of data was performed in these full contigs,
688 using MMSeqs2[61] with an identity cutoff of 0.999 and a (default) minimum of 80%
689 coverage. This resulted in 16205 unique "P4-like contigs". The collection of *att* sites
690 detected for the P4-like satellites in the 3 main bacterial species (described above) were
691 then used to subsequently delimit the regions in each contig that correspond to a P4-like
692 satellite. Briefly, we used blastn with the *blastn-short* option to detect the *att* sites in each
693 contig, retaining matches with ≥ 70% identity. To consider possible variation in *att* sites,
694 we did not enforce the match with both a specific *attL* and *attR* sequence, but instead
695 searched for either one of these sequences (i.e., two *attL* or two *attR* sequences would
696 suffice). We then extracted the shortest regions that correspond to nucleic sequences
697 that are surrounded by two of these *att* sequences, requesting a minimum of 5kb and a
698 maximum of 20kb in length for the whole *att*-defined region, according to the expected
699 distribution of sizes of P4-like elements. This resulted in 6039 unique P4-like replicons.
700 To confirm that these regions correspond to the expected P4-like satellites with enough
701 components, we first used Prodigal to extract the proteins, and then used SatelliteFinder
702 to characterize the putative P4s. This resulted in a total of 6026 P4-like satellites, where
703 most sequences (6001) correspond to P4-like satellites of Type A or B (Fig S1). This
704 suggests that our delimitation of P4-like regions using the known *att*-sites, whilst likely
705 conservative and resulting in the discarding of some valid elements, is appropriate to
706 properly define the regions of P4-like satellites.
707
708 ### Dereplication of P4 and P2 genomes
709
710 To dereplicate the final dataset used for the analyses, we merged the nucleotide
711 sequences from the *att*-defined P4-like satellites *in E. coli*, *K. pneumoniae* and *S. enterica*
712 with all the *att*-defined P4-like contigs from the metagenomes. We then clustered these
713 replicons using MMSeqs2 with the same identity cutoff as before (0.999) but with a
714 stricter 99% coverage threshold, to avoid the merging of elements that have only one
715 gene that is distinct. A similar approach was done for the *att*-defined P2-like prophages
716 in the 3 main bacterial species. This resulted in a final dataset of 3085 dereplicated P4-
717 like satellites and 1511 dereplicated P2-like prophages, which we use for all the analysis
718 described in the manuscript.

719

720 ## Identification of defence genes and systems

721

722 The detection of defence genes and systems were done with DefenseFinder version 2.0.0
723 (defense-finder-models database v2.02)[19], using the default options. We included the
724 flag -a to detect the anti-defence systems as well, albeit none were detected in P4-like
725 satellites, and very few in P2-like prophage (see main text for details). We used PADLOC
726 version 2.0.0[20] to complement the detection of complete defence systems by
727 DefenseFinder. To retrieve genes associated with putative defence systems, we extracted
728 the best hit for each gene from the *.hmmer.tsv output file of DefenseFinder.

729

730 To identify the gene repertoire of defence systems in the bacterial hosts of P4 (restricted
731 to P4 detected in complete bacterial genomes) and P2 elements, we identified the
732 defence systems in the bacterial genomes of the three main species (*E. coli, K.*
733 *pneumoniae* and *S. enterica*) that encoded at least one P4 and/or one P2, using the same
734 approaches as above. The defence gene families in bacterial hosts were computed by
735 collecting, for each species, the genes of the defence systems (either in DefenseFinder
736 or PADLOC) and clustering all the corresponding protein sequences using MMSeqs2
737 (again, the clustering was performed per each of the three species, and for each dataset,
738 DefenseFinder or PADLOC individually). A defence gene family was considered to be
739 associated with P4 or with P2 if at least one of the genes of the family is within an *att*-
740 defined P4 or P2 genome of the three main species.

741

742 ## Calculation of P4 and P2 pangenome accumulation curves

743

744 We first clustered at 40% identity all proteins of the dereplicated P4 satellites, and all
745 proteins of the dereplicated P2 prophages, using the MMSeq2 cluster function, with the
746 parameters cluster_mode 1 and the default coverage. Then, for each category of
747 elements (P4 or P2), we randomized the order of the elements and calculated the number
748 of new gene families added by each consecutive element, annotating whether their
749 representative sequences correspond to a defence-associated gene or a core gene of the
750 respective element.

Calculation of genomic similarity between P4-like satellites and between P2-like prophages

We searched for sequence similarity between all proteins of satellites using MMseqs2 with the sensitivity parameter set at 7.5 to align all versus all proteins. For specific datasets (core or defence genes), the datasets were limited to the genes that were annotated with the specific core markers or identified as defence-associated. We then performed the combinations between different datasets as well (e.g., defence vs core or defence vs whole proteome). The outputs of MMSeqs2 were converted to the blast format and we kept for analysis the hits respecting the following thresholds: e-value lower than 0.0001, at least 35% identity, and a coverage of at least 50% of the proteins (since MMSeqs2 searches for local similarity). The hits were used to retrieve the bi-directional best hits between pair of genomes, which were in turn used to compute a score of gene repertoire relatedness weighted by sequence identity:

$$wGRR = \frac{\sum_i^p id(A_i, B_i)}{\min(A, B)}$$

where A_i and B_i is the pair *I* of homologous proteins present in *A* and *B*, id(A_i,B_i) is their sequence identity in the local alignment, and min(*A*,*B*) is the number of proteins of the genome encoding the fewest proteins (*A* or *B*). wGRR is the fraction of bi-directional best hits between two genomes weighted by the sequence identity of the homologs. It varies between zero (no bi-directional best hits) and one (all genes of the smallest genome have an identical homolog in the largest genome). Hence, a wGRR=1 means that the two elements are identical (or one is entirely contained within the other), whereas wGRR=0 means the elements have no homologous protein-coding genes. wGRR integrates information on the frequency of homologs and sequence identity. For example, when the smallest genome has 10 proteins, a wGRR of 0.2 can result from two identical homologs or five homologs each with a lower sequence similarity (40%). All wGRR calculations in the manuscript were obtained through GRIS version 2 (https://gitlab.pasteur.fr/jgugliel/gris).

782 ## Calculation of the pairwise similarity of core genes of P4 or P2

783

784 To calculate the pairwise similarity between each core gene, we first collected and
785 concatenated in a fasta file all the individual core genes of P4-like satellites (7 core genes)
786 and P2-like prophages (7 core genes). Each of these files with concatenated proteins was
787 simultaneously used as both query and target database in Diamond BlastP, in order to
788 retrieve the best pairwise matches. The parameters used were the following: --query-
789 cover 50, --ultra-sensitive and --max-target-seqs 0. We then retrieved the best matches
790 for each core gene between each pair of elements.

791

792 ## Identification of pseudogenes

793

794 Pseudogenes were detected using PseudoFinder version 1.1.0[25], using the default
795 parameters. We first generated the GenBank files from the sequences to be analysed (P4-
796 like satellites, P2-like prophages, or uncharacteristic genomic regions of bacterial
797 genomes). We used as a reference database the complete set of bacterial proteins from
798 the RefSeq bacterial collection used in this study (see Bacterial genomic and
799 metagenomic datasets). We then analysed the putative pseudogenes reported by
800 PseudoFinder either as an existing ORFs or as an intergenic region predicted to be a
801 pseudogene. To functionally annotate the latter, we used the ORF from the RefSeq
802 bacterial dataset that better matches each intergenic sequenced (as reported by
803 PseudoFinder, using BlastX). The putative pseudogenes (ORFs and intergenic) were then
804 functionally annotated with the HMM profiles corresponding to the P4 and P2 core genes
805 and analysed with DefenseFinder and PADLOC to detect defence-associated genes.
806 Additionally, we annotated the pseudogenes using EggNoggMapper version 2.1.12[62], with
807 the -m diamond parameter and with all the other parameters left as default.

808

809 ## Cloning of candidate defence systems

810

811 Putative defence systems, as well as unknown P4 genes, were synthesized with their
812 native promoter and cloned into the low-copy plasmid pFR66, which carries a pSC101
813 origin of replication, a kanamycin resistance cassette, and a superfolder GFP gene under

814 the control of a pTet promoter[10]. Thus, the GFP was replaced by the candidate defence
815 systems, placing them under the control of the anhydrotetracycline (aTc) inducible pTet
816 promoter. Fifty µl of *E. coli* K-12 MG1655 chemically competent cells prepared by
817 rubidium chloride method were transformed by heat shock at 42°C with one µl of plasmid
818 carrying the candidate defence system. After 1 h of recovery at 37°C in LB (Lysogeny
819 broth) medium, transformants were selected on LB plates supplemented with
820 kananamycin (Kan) at 50 µg/ml. All constructions were verified by Nanopore sequencing.
821 The fragments of candidate defence genes are shown in Dataset E1, whilst the complete
822 plasmid sequences are shown in Dataset E2.
823
824 ## Phage amplification
825
826 The panel of 28 phages tested, including both classical model phages and a
827 representative selection of phages from the BASEL collection[63], as well as the $T5_{Mos}$
828 phage[64], was amplified on *E. coli* K-12 MG1655. For amplification of phage stocks from -
829 80°C, a frozen piece of phage stock mixed with 200 µl of an overnight culture of *E. coli* and
830 20 mL of warm (56°C) LB + CaCl2 5 mM + 0.5% agar was poured onto square plates (12 x
831 12 cm) containing LB + CaCl2 5 mM + 1% agar and incubated overnight at 37°C except for
832 the T7-like phages that were incubated at room temperature. The top-agar layer was
833 recovered with 1 mL of PBS 1X from plates on which confluent lysis was observed and
834 transferred into a 50 mL conical tube. The top agar was then disrupted by vortexing until
835 broken into small pieces. Tubes were then left to incubate 10 min at room temperature
836 before centrifugation at 4,000 g for 5 min. Finally, the supernatant was recovered and
837 filtered with a 0.45 µM filter. The phage lysates were stored at 4°C. To determine the titer
838 of the phage lysates, the lysates were serially diluted and spotted onto lawns of *E. coli*
839 MG1655.
840
841 ## Phage plaque assays
842
843 *E. coli* K-12 MG1655 strains carrying each putative defence system or the control plasmid
844 pFR66 were grown overnight in LB supplemented with Kan 50 µg/ml. Bacterial lawns were
845 prepared by mixing 200 µL of a stationary culture with 100 µl of 1 mM CaCl2 and 20 mL of

846 LB containing 0.5% agar, and the mixture was poured onto square plates (12 x 12 cm) of
847 LB supplemented with Kan 50 µg/ml with or without 0.5 µg/ml aTc. Serial dilutions of high-
848 titre (>10^8 pfu/mL) phage stocks were spotted onto each plate and incubated overnight
849 at 37°C or at room temperature for T7-like phages. The next day, plaques were counted,
850 and fold resistance was calculated as the number of plaques in the presence of each
851 system divided by the number of plaques on the control plate. When plaques were too
852 small to be counted individually, the highest-concentration dilution showing no visible
853 plaques was conservatively scored as containing a single plaque.
854
855 Machine learning detection of antiviral domains in P4-like satellites and annotation of
856 novel defence systems
857
858 To annotate the candidate defence systems and characterize potential antiviral domains,
859 sequence and structural homology analyses were performed. Sequence homology was
860 first assessed using Pfam-A annotation using PyHMMER[65] (v0.11), a Pyhton library
861 binding to HMMER[66] (v3.4). To annotate protein regions without Pfam annotations,
862 HHpred[67] was used with 3 iterations on Pfam-A (online version) to identify conserved
863 domains via profile-to-profile Hidden Markov Model (HMM) comparisons. Structural
864 predictions were used for both homology detection and representation. For homology
865 detection, 3D protein models were generated using ESM-Fold, and the resulting PDB files
866 were processed through the Foldseek web server[68] to identify structural homologs within
867 the PDB and AlphaFold databases. In the second approach, AlphaFold 3.0.1 was
868 employed to generate structural predictions, evaluating monomeric or dimeric
869 configurations (when the system has 2 genes). When possible, we annotated whether the
870 novel systems were predicted as potentially defensive[69] (GeneCLR hit in File S3). These
871 integrated structural data were used to infer the presence of specialized antiviral effector
872 or sensor domains by comparing the predicted folds to known defence-related protein
873 architectures.
874
875 Genes of unknown functions were scored by both the ESM-650M_{DF} and the
876 geneCLR$_{DF}$ scores as defined in[69]. The methods were run on representative sequences

877 when clustering the database at 95% of identity. Thus, we mapped the genes of unknown
878 function to their representative 95 and retrieved the corresponding scores.
879
880 ## Detection of homologs of P4/P2 defence genes in bacterial and bacteriophage genomes
881
882 We collected all defence-associated proteins in P4-like satellites and P2-like genomes,
883 and then used this set with Diamond BlastP to search for homologs in the complete
884 RefSeq bacterial genomes, including their plasmids. We used Diamond BlastP with the
885 parameters --query-cover 50, --ultra-sensitive and --max-target-seqs 0. We then
886 retrieved all matches with at least 85% identity with the query sequence and consider
887 these as homologs of the matched defence genes. We did a similar analysis to search for
888 homologs of P4 or P2 defence-associated proteins in the dataset of 27022 bacteriophage
889 genomes described above.
890
891 The genomic context of the homologs detected in bacterial genomes is assigned as a
892 plasmid (if in a secondary replicon of the bacterial genome), a prophage (if in a region
893 detected as such by geNomad), a satellite (if in a region detected as such by
894 SatelliteFinder), a phage-plasmid (if the plasmid replicon correspond to known phage-
895 plasmids[37] or if geNomad detects a secondary replicon as a prophage) or an integrative
896 mobile element (i.e., Integrative Conjugative Elements – ICEs –, Integrative Mobilizable
897 Elements – IMEs – or iOriTs, if in a region detected as described in[34]). If the defence
898 homolog was detected in a bacterial genomic region that does not correspond to any of
899 the categories above, we assigned it as an "uncharacteristic genomic region".
900
901 To account for the possibility that homology of defence systems is caused by vertical
902 descent within the element, i.e., cases where an homolog of a P4/P2 defence gene was
903 found in a bacterial region that corresponds to that same P4/P2, we calculated the core
904 (minus the integrase) wGRR (see section above) between all P4 and P4*, and all P2 and
905 P2*, and discarded homologous matches with elements that had a wGRR of at least 0.95.
906
907 ## Phylogenetic analyses
908

909 To compute the phylogenies of P4 and P2 elements, we extracted all their respective core
910 proteins (except for the integrase), and aligned each set of proteins individually, using
911 using mafft-linsi[70] (v. 7.490, default parameters). The individual alignments of core
912 proteins were then concatenated in two alignments (one with the P4 core proteins,
913 another with the P2 core proteins). For elements where some core genes were missing, a
914 sequence of gaps ("-") was added. The resulting alignment was trimmed with clipkit[71] (v.
915 1.3.0, default parameters). We then used IQ-Tree[72] (v. 1.6.12) to build the phylogenetic
916 trees, with the options –bb 1000 to run the ultrafast bootstrap option with 1000 replicates
917 and -m TEST option for automatic model choice . The resulting tree files were visualized
918 and edited using the v5 webserver of iTOL[73]
919
920 The phylogenies of individual defence genes were inferred by aggregating in single fasta
921 files all the protein sequences corresponding to homologous matches of specific
922 defence genes (PD-T7-2, Lit and Avs_V). Systems with more than one gene (i.e., PD-T7-2)
923 were aggregated in separate files, and each gene was processed separately. The
924 alignments and phylogenies were assembled and visualized as described above.
925
926 ## Functional annotation of uncharacteristic genomic regions
927
928 Homologous matches of defence genes of P4/P2 in bacterial chromosomic regions that
929 do not correspond to known MGEs were defined as "uncharacteristic genomic regions".
930 To analyse the genomic context of these homolog genes, we extracted 20 genes upstream
931 and 20 genes downstream. These regions were then further annotated with
932 DefenseFinder[19] and PADLOC[20], P4 and P2-specific HMM markers, and EggNogMapper[62],
933 all with the same parameters described above in each section. We also used
934 PseudoFinder[25], as described above, to detect pseudogenes in these uncharacteristic
935 genomic regions, and the intergenic pseudogenes detected were further classified with
936 P4 and P2 specific HMM profiles. To maintain specificity, we excluded from the search for
937 core markers the integrase of P4/P2, as well as Delta and AlpA of P4, since homologs to
938 these components can be found in other MGEs.
939
940 ## Visualization of genomic regions

Genome visualization across the manuscript uses Clinker version 0.0.3[74] with the -i parameter set at 0.3 at the other parameters were left as default. The JSON output files were edited to better represent the colors of the gene clusters.

Acknowledgements

We thank all the Microbial Evolutionary Genomics Unit members for the regular discussions throughout the project. The authors also wish to acknowledge the students of the 2025 M2 Microbiology course at Institut Pasteur (Pierric Chuppa, Hugo Cibla, Léa Dunand-Sauthier, Esteban Francois, Thibault Frisch, Theana Gardais, Chiara Gouviaux-Deletraz, Dorian Joffres, Ekaterina Korotaeva, Kevin Koule, Jeane Le Floch, Nicolas Le Jalle, Laly Meyer, Laura Ochsenbein, Orane Pion, Maël Rochefort, Corentin Rohel, Alexandre Roubaud, Inès Santos and Sofia Tagkalidou), who collaborated in the preliminary assays of infection the candidate defence systems. This work used the computational and storage services (MAESTRO cluster) provided by the IT department at Institut Pasteur, Paris. We acknowledge support from the Laboratoire d'Excellence IBEID Integrative Biology of Emerging Infectious Diseases [ANR-10-LABX-62-IBEID], the Agence Nationale de Recherche [ANR 23 CE20 0046 01 TRIADE] and [ANR-20-CE12-0004 TransfoConflict] and the HORIZON programme [HORIZON-MSCA-2024-PF-01 TriSH]. This work used the computational and storage services (MAESTRO cluster) provided by the IT department at Institut Pasteur, Paris.

REFERENCES

1. Clokie, M. R. J., Millard, A. D., Letarov, A. V. & Heaphy, S. Phages in nature. *Bacteriophage* **1**, 31–45 (2011).
2. Touchon, M., Moura de Sousa, J. A. & Rocha, E. P. Embracing the enemy: the diversification of microbial gene repertoires by phage-mediated horizontal gene transfer. *Curr. Opin. Microbiol.* **38**, 66–73 (2017).
3. Shkoporov, A. N., Turkington, C. J. & Hill, C. Mutualistic interplay between bacteriophages and bacteria in the human gut. *Nat. Rev. Microbiol.* https://doi.org/10.1038/s41579-022-00755-4 (2022) doi:10.1038/s41579-022-00755-4.
4. Dedrick, R. M. *et al.* Prophage-mediated defence against viral attack and viral counter-defence. *Nat. Microbiol.* **2**, 16251 (2017).
5. Brenes, L. R. & Laub, M. T. E. coli prophages encode an arsenal of defense systems to protect against temperate phages. *Cell Host Microbe* **33**, 1004-1018.e5 (2025).
6. Beamud, B., Benz, F. & Bikard, D. Going viral: The role of mobile genetic elements in bacterial immunity. *Cell Host Microbe* **32**, 804–819 (2024).
7. Clabby, T., Tesson, F., Gaborieau, B. & Bernheim, A. Why do bacteria accumulate antiphage defence systems? *Philos. Trans. R. Soc. B Biol. Sci.* **380**, 20240082 (2025).
8. Ares-Arroyo, M., Coluzzi, C., Moura De Sousa, J. A. & Rocha, E. P. C. Hijackers, hitchhikers, or co-drivers? The mysteries of mobilizable genetic elements. *PLOS Biol.* **22**, e3002796 (2024).
9. Penadés, J. R., Seed, K. D., Chen, J., Bikard, D. & Rocha, E. P. C. Genetics, ecology and evolution of phage satellites. *Nat. Rev. Microbiol.* **23**, 410–422 (2025).

10. Rousset, F. *et al.* Phages and their satellites encode hotspots of antiviral systems. *Cell Host Microbe* **30**, 740-753.e5 (2022).

11. Puigbò, P., Makarova, K. S., Kristensen, D. M., Wolf, Y. I. & Koonin, E. V. Reconstruction of the evolution of microbial defense systems. *BMC Evol. Biol.* **17**, 94 (2017).

12. Hussain, F. A. *et al.* Rapid evolutionary turnover of mobile genetic elements drives bacterial resistance to phages. *Science* **374**, 488–492 (2021).

13. Hatfull, G. F. Bacteriophage genomics. *Curr. Opin. Microbiol.* **11**, 447–453 (2008).

14. Dion, M. B., Oechslin, F. & Moineau, S. Phage diversity, genomics and phylogeny. *Nat. Rev. Microbiol.* **18**, 125–138 (2020).

15. Kindt, J., Tzlil, S., Ben-Shaul, A. & Gelbart, W. M. DNA packaging and ejection forces in bacteriophage. *Proc. Natl. Acad. Sci.* **98**, 13671–13674 (2001).

16. Leclercq, S. & Cordaux, R. Do phages efficiently shuttle transposable elements among prokaryotes? *Evolution* **65**, 3327–3331 (2011).

17. de Sousa, J. A. M., Fillol-Salom, A., Penadés, J. R. & Rocha, E. P. C. Identification and characterization of thousands of bacteriophage satellites across bacteria. *Nucleic Acids Res.* gkad123 (2023) doi:10.1093/nar/gkad123.

18. Chikhi, R. *et al.* Logan: Planetary-Scale Genome Assembly Surveys Life's Diversity. Preprint at https://doi.org/10.1101/2024.07.30.605881 (2024).

19. Tesson, F. *et al.* Systematic and quantitative view of the antiviral arsenal of prokaryotes. *Nat. Commun.* **13**, 2561 (2022).

20. Payne, L. J. *et al.* PADLOC: a web server for the identification of antiviral defence systems in microbial genomes. *Nucleic Acids Res.* **50**, W541–W550 (2022).

1010 21. Fillol-Salom, A. *et al.* Bacteriophages benefit from mobilizing pathogenicity
1011 islands encoding immune systems against competitors. *Cell* **185**, 3248-3262.e20
1012 (2022).
1013 22. Christie, G. E. & Calendar, R. Bacteriophage P2. *Bacteriophage* **6**, e1145782
1014 (2016).
1015 23. Nilsson, A. S. & Haggård-Ljungquist, E. Evolution of P2-like phages and their
1016 impact on bacterial evolution. *Res. Microbiol.* **158**, 311–317 (2007).
1017 24. Egorov, A. A., Hauryliuk, V. & Atkinson, G. C. Systematic annotation of hyper-
1018 variability hotspots in phage genomes and plasmids. Preprint at
1019 https://doi.org/10.1101/2024.10.15.618418 (2024).
1020 25. Syberg-Olsen, M. J., Garber, A. I., Keeling, P. J., McCutcheon, J. P. & Husnik, F.
1021 Pseudofinder: Detection of Pseudogenes in Prokaryotic Genomes. *Mol. Biol. Evol.* **39**,
1022 msac153 (2022).
1023 26. Mariano, G. & Blower, T. R. Conserved domains can be found across distinct
1024 phage defence systems. *Mol. Microbiol.* **120**, 45–53 (2023).
1025 27. Georjon, H. & Bernheim, A. The highly diverse antiphage defence systems of
1026 bacteria. *Nat. Rev. Microbiol.* **21**, 686–700 (2023).
1027 28. Haudiquet, M. *et al.* Structural basis for Lamassu-based antiviral immunity and
1028 its evolution from DNA repair machinery. *Proc. Natl. Acad. Sci.* **122**, e2519643122
1029 (2025).
1030 29. Gorbalenya, A. E. & Koonin, E. V. Endonuclease (R) subunits of type-I and type-III
1031 restriction-modification enzymes contain a helicase-like domain. *FEBS Lett.* **291**,
1032 277–281 (1991).

1033 30. Gao, L. *et al.* Diverse enzymatic activities mediate antiviral immunity in
1034 prokaryotes. *Science* **369**, 1077–1084 (2020).
1035 31. Liu, H. W., Roisné-Hamelin, F. & Gruber, S. SMC-based immunity against
1036 extrachromosomal DNA elements. *Biochem. Soc. Trans.* **51**, 1571–1583 (2023).
1037 32. Andersen, S. E. *et al.* Serine recombinases are conserved genetic markers of
1038 antiphage defense systems. Preprint at https://doi.org/10.1101/2025.10.07.681051
1039 (2025).
1040 33. Tan, J. M. J. *et al.* A DNA-gated molecular guard controls bacterial Hailong anti-
1041 phage defence. *Nature* **643**, 794–800 (2025).
1042 34. Ares-Arroyo, M., Junker, R., Nucci, A., Touchon, M. & Rocha, E. P. C. Genomic
1043 Islands as minimal hitchers of conjugative elements. Preprint at
1044 https://doi.org/10.64898/2026.01.13.699239 (2026).
1045 35. Johnson, C. M., Harden, M. M. & Grossman, A. D. Interactions between mobile
1046 genetic elements: An anti-phage gene in an integrative and conjugative element
1047 protects host cells from predation by a temperate bacteriophage. *PLOS Genet.* **18**,
1048 e1010065 (2022).
1049 36. Camargo, A. P. *et al.* Identification of mobile genetic elements with geNomad.
1050 *Nat. Biotechnol.* **42**, 1303–1312 (2024).
1051 37. Pfeifer, E., Moura de Sousa, J. A., Touchon, M. & Rocha, E. P. C. Bacteria have
1052 numerous distinctive groups of phage–plasmids with conserved phage and variable
1053 plasmid gene repertoires. *Nucleic Acids Res.* **49**, 2655–2673 (2021).
1054 38. Reiter, W.-D., Palm, P. & Yeats, S. Transfer RNA genes frequently serve as
1055 integration sites for prokaryotic genetic elements. *Nucleic Acids Res.* **17**, 1907–1914
1056 (1989).

39. Aframian, N., Omer Bendori, S., Hen, T., Guler, P. & Eldar, A. Expression level of anti-phage defence systems controls a trade-off between protection range and autoimmunity. *Nat. Microbiol.* **10**, 1954–1962 (2025).

40. Frumkin, I., Vassallo, C. N., Chen, Y. H. & Laub, M. T. Emergence of antiphage functions from random sequence libraries reveals mechanisms of gene birth. *Proc. Natl. Acad. Sci.* **122**, e2513255122 (2025).

41. Christie, G. E. & Calendar, R. INTERACTIONS BETWEEN SATELLITE BACTERIOPHAGE P4 AND ITS HELPERS. *Annu. Rev. Genet.* **24**, 465–490 (1990).

42. Lindqvist, B. H., Dehò, G. & Calendar, R. Mechanisms of genome propagation and helper exploitation by satellite phage P4. *Microbiol. Rev.* **57**, 683–702 (1993).

43. Smith, G. R. Chi hotspots of generalized recombination. *Cell* **34**, 709–710 (1983).

44. Mosig, G. Recombination and recombination-dependent DNA replication in bacteriophage T4. *Annu. Rev. Genet.* **32**, 379–413 (1998).

45. Vulić, M., Dionisio, F., Taddei, F. & Radman, M. Molecular keys to speciation: DNA polymorphism and the control of genetic exchange in enterobacteria. *Proc. Natl. Acad. Sci.* **94**, 9763–9767 (1997).

46. Moura de Sousa, J. A., Pfeifer, E., Touchon, M. & Rocha, E. P. C. Causes and Consequences of Bacteriophage Diversification via Genetic Exchanges across Lifestyles and Bacterial Taxa. *Mol. Biol. Evol.* **38**, 2497–2512 (2021).

47. Koonin, E. V., Makarova, K. S., Wolf, Y. I. & Krupovic, M. Evolutionary entanglement of mobile genetic elements and host defence systems: guns for hire. *Nat. Rev. Genet.* **21**, 119–131 (2020).

48. Sheinman, M. *et al.* Identical sequences found in distant genomes reveal frequent horizontal transfer across the bacterial domain. *eLife* **10**, e62719 (2021).

1081 49. Oliveira, P. H., Touchon, M., Cury, J. & Rocha, E. P. C. The chromosomal
1082 organization of horizontal gene transfer in bacteria. *Nat. Commun.* **8**, 841 (2017).
1083 50. Baker, J., Limberger, R., Schneider, S. J. & Campbell, A. Recombination and
1084 modular exchange in the genesis of new lambdoid phages. *New Biol.* **3**, 297–308
1085 (1991).
1086 51. Dragoš, A. *et al.* Pervasive prophage recombination occurs during evolution of
1087 spore-forming *Bacilli*. *ISME J.* **15**, 1344–1358 (2021).
1088 52. Touchon, M. *et al.* Phylogenetic background and habitat drive the genetic
1089 diversification of Escherichia coli. *PLOS Genet.* **16**, e1008866 (2020).
1090 53. Buchfink, B., Reuter, K. & Drost, H.-G. Sensitive protein alignments at tree-of-life
1091 scale using DIAMOND. *Nat. Methods* **18**, 366–368 (2021).
1092 54. Hockenberry, A. J. & Wilke, C. O. BACPHLIP: predicting bacteriophage lifestyle
1093 from conserved protein domains. *PeerJ* **9**, e11396 (2021).
1094 55. Néron, B. *et al.* MacSyFinder v2: Improved modelling and search engine to
1095 identify molecular systems in genomes. *Peer Community J.* **3**, e28 (2023).
1096 56. Casjens, S. R. & Grose, J. H. Contributions of P2- and P22-like prophages to
1097 understanding the enormous diversity and abundance of tailed bacteriophages.
1098 *Virology* **496**, 255–276 (2016).
1099 57. Perrin, A. & Rocha, E. P. C. PanACoTA: a modular tool for massive microbial
1100 comparative genomics. *NAR Genomics Bioinforma.* **3**, lqaa106 (2021).
1101 58. Rajeev, L., Malanowska, K. & Gardner, J. F. Challenging a paradigm: the role of
1102 DNA homology in tyrosine recombinase reactions. *Microbiol. Mol. Biol. Rev. MMBR*
1103 **73**, 300–309 (2009).

1104 59. Camacho, C. *et al.* BLAST+: architecture and applications. *BMC Bioinformatics*
1105 **10**, 421 (2009).
1106 60. Mageeney, C. M. *et al.* New candidates for regulated gene integrity revealed
1107 through precise mapping of integrative genetic elements. *Nucleic Acids Res.* **48**,
1108 4052–4065 (2020).
1109 61. Steinegger, M. & Söding, J. MMseqs2 enables sensitive protein sequence
1110 searching for the analysis of massive data sets. *Nat. Biotechnol.* **35**, 1026–1028
1111 (2017).
1112 62. Cantalapiedra, C. P., Hernández-Plaza, A., Letunic, I., Bork, P. & Huerta-Cepas, J.
1113 eggNOG-mapper v2: Functional Annotation, Orthology Assignments, and Domain
1114 Prediction at the Metagenomic Scale. *Mol. Biol. Evol.* **38**, 5825–5829 (2021).
1115 63. Maffei, E. *et al.* Systematic exploration of Escherichia coli phage–host
1116 interactions with the BASEL phage collection. *PLOS Biol.* **19**, e3001424 (2021).
1117 64. Burman, N. *et al.* A virally encoded tRNA neutralizes the PARIS antiviral defence
1118 system. *Nature* **634**, 424–431 (2024).
1119 65. Larralde, M. & Zeller, G. PyHMMER: a Python library binding to HMMER for
1120 efficient sequence analysis. *Bioinformatics* **39**, btad214 (2023).
1121 66. Eddy, S. R. Accelerated Profile HMM Searches. *PLoS Comput. Biol.* **7**, e1002195
1122 (2011).
1123 67. Gabler, F. *et al.* Protein Sequence Analysis Using the MPI Bioinformatics Toolkit.
1124 *Curr. Protoc. Bioinforma.* **72**, e108 (2020).
1125 68. Van Kempen, M. *et al.* Fast and accurate protein structure search with Foldseek.
1126 *Nat. Biotechnol.* **42**, 243–246 (2024).

69. Mordret, E. *et al*. Protein and genomic language models chart a vast landscape of antiphage defenses. Preprint at https://doi.org/10.1101/2025.01.08.631966 (2025).

70. Katoh, K. & Standley, D. M. MAFFT Multiple Sequence Alignment Software Version 7: Improvements in Performance and Usability. *Mol. Biol. Evol.* **30**, 772–780 (2013).

71. Steenwyk, J. L., Buida, T. J., Li, Y., Shen, X.-X. & Rokas, A. ClipKIT: A multiple sequence alignment trimming software for accurate phylogenomic inference. *PLOS Biol.* **18**, e3001007 (2020).

72. Nguyen, L.-T., Schmidt, H. A., von Haeseler, A. & Minh, B. Q. IQ-TREE: A Fast and Effective Stochastic Algorithm for Estimating Maximum-Likelihood Phylogenies. *Mol. Biol. Evol.* **32**, 268–274 (2015).

73. Letunic, I. & Bork, P. Interactive Tree Of Life (iTOL) v5: an online tool for phylogenetic tree display and annotation. *Nucleic Acids Res.* **49**, W293–W296 (2021).

74. Gilchrist, C. L. M. & Chooi, Y.-H. clinker & clustermap.js: automatic generation of gene cluster comparison figures. *Bioinformatics* **37**, 2473–2475 (2021).